Adiabatic cooling for cold polar molecules on a chip using a controllable high-efficiency electrostatic surface trap*

Li Sheng-Qiang(李胜强), Xu Liang(许 亮), Xia Yong(夏 勇),
Wang Hai-Ling(汪海玲), and Yin Jian-Ping(印建平)†

State Key Laboratory of Precision Spectroscopy, Department of Physics, East China Normal University, Shanghai 200062, *China*

(Received 18 April 2014; revised manuscript received 23 June 2014; published online 10 October 2014)

We propose a controllable high-efficiency electrostatic surface trap for cold polar molecules on a chip by using two insulator-embedded charged rings and a grounded conductor plate. We calculate Stark energy structure pattern of ND_3 molecules in an external electric field using the method of matrix diagonalization. We analyze how the voltages that are applied to the ring electrodes affect the depth of the efficient well and the controllability of the distance between the trap center and the surface of the chip. To obtain a better understanding, we simulate the dynamical loading and trapping processes of ND_3 molecules in a $|J,KM\rangle = |1,-1\rangle$ state by using classical Monte–Carlo method. Our study shows that the loading efficiency of our trap can reach $\sim 88\%$. Finally, we study the adiabatic cooling of cold molecules in our surface trap by linearly lowering the potential-well depth (i.e., lowering the trapping voltage), and find that the temperature of the trapped ND_3 molecules can be adiabatically cooled from 34.5 mK to ~ 5.8 mK when the trapping voltage is reduced from -35 kV to -3 kV.

Keywords: controllable, high-efficiency, surface trap, cold polar molecules

PACS: 37.10.Pq, 37.10.Mn, 37.10.Vz, 37.20.+j **DOI:** 10.1088/1674-1056/23/12/123701

1. Introduction

Cold molecules have a wide range of applications in applied physics,[1–5] such as high-resolution spectroscopy and precision measurements,[6] conformer separation and orientation,[7] cold collisions and cold chemistry,[8–10] etc. Many ingenious methods to prepare cold molecules were proposed, such as laser cooling,[11,12] photoassociation,[13–15] Feshbach resonance,[16–18] buffer-gas cooling,[19,20] velocity filters,[21] electrostatic Stark deceleration,[22–25] Rydberg deceleration,[26] Zeeman deceleration,[27–29] optical Stark deceleration,[30,31] collisions or reactions,[32,33] and mechanical method,[34] and so on. Manipulation of cold polar molecules using the interaction of their electric dipole moments with an inhomogeneous electric field has obtained great achievements in recent years. For example, a Stark decelerator can be used to slow the velocity of a supersonic molecular beam to a standstill and obtain a cold molecular packet with a translational temperature in a range of about 3 mK–30 mK,[22–25] an electrostatic potential well can be used to trap the slowed cold molecules.[35] Trapped cold molecules can be used in many fields. For example, if cold molecules can be trapped in a potential well for up to seconds, the lifetimes of its excited electronic or vibrational states can be studied.[36,37] Trapped polar molecules hold promise for applications in quantum computing and information processing.[38] Trapped cold molecular gases are suitable to study molecular interactions, collective effects, and realize molecular Bose–Einstein condensation in experiments. Since the first electrostatic trap for the Stark-decelerated ND_3 molecules was demonstrated in 2000 by Bethlem *et al*., various kinds of electrostatic traps have been developed for cold polar molecules in both the weak-field-seeking (WFS) state and the strong-field-seeking (SFS) state.[39–43] In particular, trapping molecules on a chip has some interesting phenomena, for example, the reduction of the trapping lifetime due to the heating of the molecules by interaction with the surface can be studied as a function of temperature and distance from the surface.[44] Remarkable trapping scheme reported by the Meijer *et al*. was the trapping of carbon monoxide molecules on a chip using direct loading from a supersonic beam.[45] Another two electrostatic surface trap schemes were proposed by our group,[46,47] but there are two disadvantages in these schemes: one is that the position of the trapping center of cold molecules cannot be controlled by adjusting the voltage on the ring electrode when all geometric parameters of the surface trap scheme are given, and the other is that the loading efficiency of cold molecules is no more than 12%, according to their Monte–Carlo simulations.

In this paper, to solve these problems, we propose a con-

*Project supported by the National Natural Science Foundation of China (Grant Nos. 10674047, 10804031, 10904037, 10904060, 10974055, 11034002, and 61205198), the National Key Basic Research and Development Program of China (Grant Nos. 2006CB921604 and 2011CB921602), the Basic Key Program of Shanghai Municipality, China (Grant No. 07JC14017), the Fundamental Research Funds for the Central Universities, and the Shanghai Leading Academic Discipline Project, China (Grant No. B408).

†Corresponding author. E-mail: jpyin@phy.ecnu.edu.cn

© 2014 Chinese Physical Society and IOP Publishing Ltd

trollable high-efficiency electrostatic surface trap for cold polar molecules in the WFS states on a chip, and demonstrate the feasibility of our surface trap scheme by using classical Monte–Carlo simulations. The rest of this paper is arranged as follows. In Section 2, a controllable high-efficiency electrostatic surface trap for cold polar molecules on a chip is proposed. We calculate Stark energy structure pattern of ND_3 molecules in an external electric field using the method of matrix diagonalization. We also analyze how the voltages that are applied to the ring electrodes affect the depth of the efficient well and the controllability of the distance between the trap center and the surface of the chip. In Section 3, we perform the classical Monte–Carlo simulations to better understand the dynamic behavior of cold molecules in the processes of molecular loading and trapping. In Section 4, we use our trap scheme to study the adiabatic cooling of the trapped ND_3 molecules. In the final section, we summarize some main results and draw conclusions from the present study.

2. Electrostatic surface trap and its field calculation

2.1. Electrostatic surface trap scheme

The schematic diagram of our proposed electrostatic surface trap is shown in Fig. 1(a). Two insulating substrates are made of teflon (relative permittivity $\varepsilon_r = 2.1$) plates, and the thickness values of the substrate 1 and 2 are a and b, respectively. In our scheme, there are two stainless steel ring electrodes with a curvature radius R, and they will be formed by bending three stainless steel wires each with a radius r_0. The ring 1 is embedded in an upper surface of the insulation substrate 1 by a depth r_0 (i.e., the radius of the ring), and the ring 2 is embedded between the lower surface of the substrate 1 and the upper surface of the substrate 2. The voltage U_1 is applied to the ring 1, and U_2 is applied to the ring 2, and the metal plate is grounded. The arrow in Fig. 1(a) indicates the loading direction of the incident cold molecular beam. Figure 1(b) shows the contour distribution of the electrostatic field for $a = b = 4$ mm, $r_0 = 1$ mm, $R = 4$ mm, $U_1 = -15$ kV, and $U_2 = 0$. Here Z_0 is the distance between the trap center and the surface of the chip.

In our scheme, the charged ring 1 is used to form a closed three-dimensional (3D) electrostatic trap, and its trapping center is located at the center of the ring 1 (i.e., at the surface of the chip), and its trapping central position cannot be changed. Meanwhile the charged ring 2 is used to realize both the loading of cold molecules from a cold molecular beam into our surface trap and the controlling of the trapping central position along the z direction.

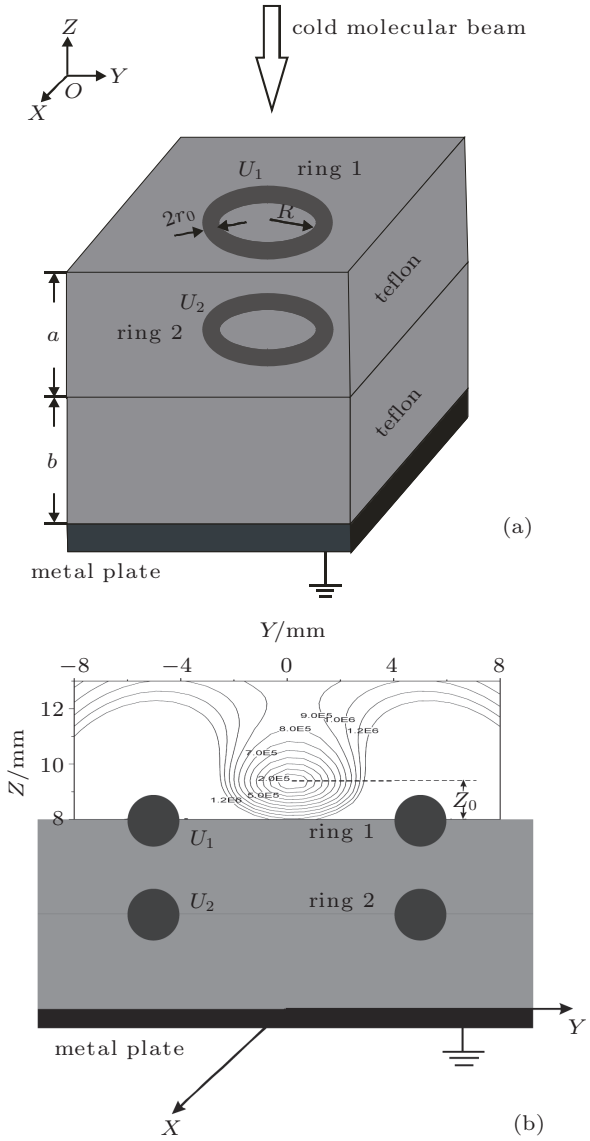


Fig. 1. (a) Schematic diagram for trapping molecules on a chip using two charged rings and a ground plate. The voltages applied to the ring 1 and ring 2 are U_1 and U_2, respectively. Two layers of teflon substrates are marked, and the thickness values of substrates 1 and 2 are a and b, respectively. The arrow indicates the loading direction of the incident molecular beam. The ring 2 is sandwiched between two pieces of the substrates. (b) Contour distribution of the electrostatic field for $a = b = 4$ mm, $r_0 = 1$ mm, $R = 4$ mm, $U_1 = -15$ kV, $U_2 = U_3 = 0$. Z_0 is the distance between the trap center and the surface of the chip. In panel (b), the electrostatic field is written in the form of 1.2E6, which means 1.2×10^6.

2.2. Calculation of electrostatic field and its Stark potential for ND_3

Here we choose ND_3 molecules as our test molecules not only because the ND_3 molecule in the state $|J, KM\rangle = |1, -1\rangle$ has a relatively large electric dipole moment (1.5 Debye) and a relatively small mass, but also because the ND_3 molecule has been successfully decelerated and trapped.[23,25] Last but not least, we can make a direct comparison of the present scheme with our previous schemes.[46,47] Now, we will calculate the Stark energy structure pattern of ND_3 molecules in an external electric field using the method of matrix diagonalization.

ND_3 is an oblate symmetric top molecule. The rotational Hamiltonian of ND_3 is

$$H_0 = BJ^2 + (C-B)J_z. \tag{1}$$

Here the wave function is $|JKM\rangle$ and

$$|JKM\rangle = \sqrt{\frac{2J+1}{8\pi^2}} D^{(J)*}_{MK}(\phi,\theta,\chi), \tag{2}$$

with ϕ, θ, and χ denoting the Euler angles, which determine the orientation of the $\hat{x}$, $\hat{y}$, $\hat{z}$ axes (molecular coordinate frame) with respect to the $\hat{X}$, $\hat{Y}$, $\hat{Z}$ axes (space-fixed frame).

Here, the dipole moment and electric field vectors are represented as irreducible spherical tensor operator:[48]

$$H_{\text{Stark}} = -\boldsymbol{\mu}\cdot\boldsymbol{E} = -\sum_{p=-1}^{1}(-1)^p T_\mu(1,p)T_E(1,p), \tag{3}$$

where

$$T_\mu(1,-1) = \frac{1}{\sqrt{2}}(\mu,-\mathrm{i}\mu), \tag{4}$$

$$T_\mu(1,0) = \mu_Z, \tag{5}$$

$$T_\mu(1,1) = -\frac{1}{\sqrt{2}}(\mu,+\mathrm{i}\mu), \tag{6}$$

$$T_E(1,-1) = \frac{1}{\sqrt{2}}(E_X,E_Y), \tag{7}$$

$$T_E(1,0) = E_Z, \tag{8}$$

$$T_E(1,1) = -\frac{1}{\sqrt{2}}(E_X,E_Y). \tag{9}$$

Suppose that the space-fixed coordinate system is chosen such that the electric field vector is directed along the $\boldsymbol{Z}$ axis, then the Hamiltonian reduces to

$$H_{\text{Stark}} = -T_\mu(1,0)\cdot E. \tag{10}$$

A transformation from the space-fixed frame to the rotating molecular frame can be made with the help of the Wigner rotation matrices[48]

$$T_\mu(1,0) = \sum_{q=-1}^{1} D^{(1)*}_{0q}(\phi,\theta,\chi)\tilde{T}_\mu(1,q), \tag{11}$$

$H = H_0 + H_{\text{Stark}}$. Considering the inversion splitting, we incorporate the parity into the wave function. The matrix elements are as follows:

$$\begin{aligned}
&\langle JKM\pm|H|J'K'M'\mp\rangle \\
&= \langle JKM|H|J'K'M'\rangle \\
&= -E\sqrt{(2J+1)(2J'+1)}\sum_q(-1)^{M-K}\tilde{T}_\mu(1,q) \\
&\quad\times\begin{pmatrix} J & 1 & J' \\ M & 0 & -M' \end{pmatrix}\begin{pmatrix} J & 1 & J' \\ K & -q & -K' \end{pmatrix}.
\end{aligned} \tag{12}$$

Then we obtain the Stark energy level diagrams of the rotational states for ND_3 molecule which is shown in Fig. 2 through programming. The dashed line shown in Fig. 2(b) is the approximate solution obtained from the approximate formula[3]

$$E_{\text{Stark}} = \frac{E_{\text{inv}}}{2} \pm \sqrt{\left(\frac{E_{\text{inv}}}{2}\right)^2 + \left(\mu E\frac{M\Omega_{\text{eff}}}{J(J+1)}\right)^2}. \tag{13}$$

As we can see, when the electric field is not too large, the approximate solution fits the exact solution well.

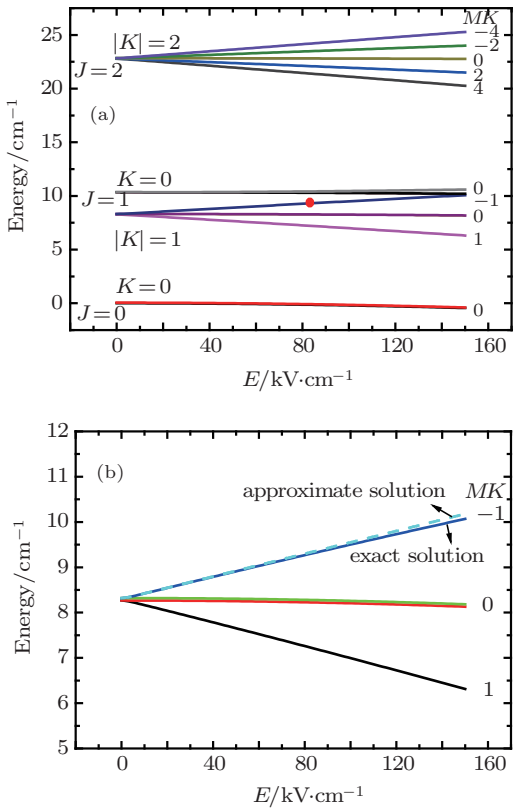


Fig. 2. (color online) (a) Stark energy structure patterns of ND_3 molecules in an external electric field for rotational quantum state of $J = 0, 1$, and 2. (b) Comparison of the Stark shift between the approximate solution and the exact solution for the rotational quantum state of $J = 1$, and $MK = -1$.

2.3. Effects of voltage on the controllability of our surface trap and the depth of effective trap

Here the space between the minimum of the electrical field and the upper surface of the substrate 1 is denoted by Z_0. In our calculation, the used parameters are as follows: $R = 4$ mm, $a = b = 4$ mm, the metal plate is grounded, and the voltage U_2 applied to the ring 2 is zero. Figure 3(a) shows the dependences of Z_0 and the depth of effective trap (W) on the voltage applied to the ring 1 (U_1). Usually, the smallest well depth in the X, Y, and Z directions is defined as the effective well depth. It is clear from Fig. 3 that as the voltage U_1 is changed from -5 kV to -35 kV, the value of Z_0 remains at 1.4 mm, while W increases from about 51.4 mK to 358.4 mK. So, we can obtain the following conclusions: the depth of the

effective trap changes with U_1 significantly while the trap center remains unchanged.

Figure 3(b) shows that as U_2 changes from negative voltage to positive voltage, the value of position Z_0 of the trapping center increases. As the voltage U_2 is varied from -8 kV to 30 kV, the value of trap-center position Z_0 will be adjusted from 0.4 mm to 2.9 mm. This shows that the height of our trap center can be conveniently controlled by changing the voltage U_2 on the ring 2. As U_2 is increased from -8 kV to 30 kV, W first rapidly increases from 41.2 mK to the maximum value (159.3 mK), then drops slowly down to 115.2 mK.

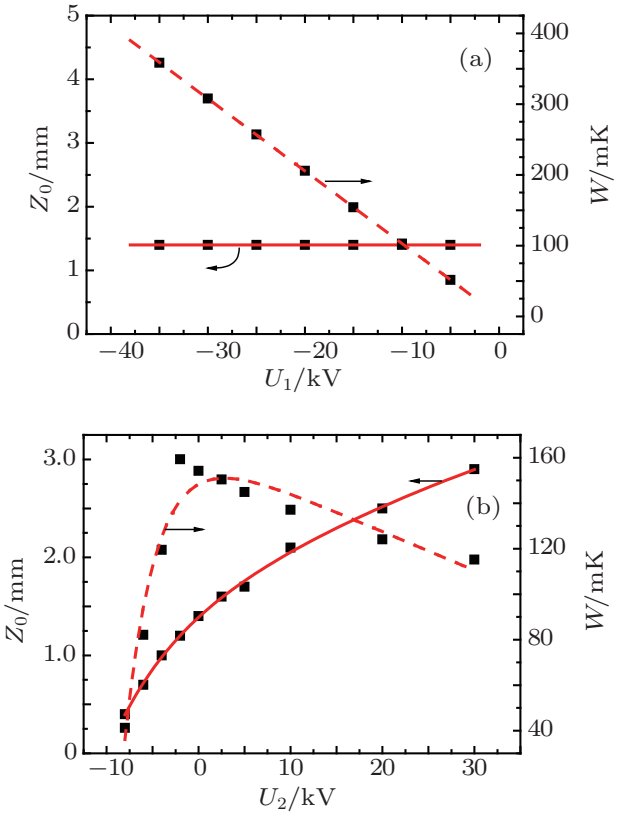


Fig. 3. (color online) (a) Relationships between Z_0 and U_1, and between W and U_1. (b) The relationships between Z_0 and U_2, and between W and U_2.

3. Numeric simulations and results

To better understand the loading and trapping behaviors of cold polar molecules from a cold molecular beam into our surface trap, we perform Monte–Carlo simulations for ND_3 molecules in the state $|J,KM\rangle = |1,-1\rangle$, and the results are shown in Figs. 4 and 5 respectively. In the process of loading, the parameters are chosen to be $a = b = 4$ mm, $r_0 = 1$ mm, $R = 4$ mm, $U_1 = -2$ kV, and $U_2 = 15$ kV, while in the process of trapping, the parameters are chosen to be $a = b = 4$ mm, $r_0 = 1$ mm, $R = 4$ mm, $U_1 = -15$ kV, and $U_2 = 0$ kV. Figure 4(a) shows the field distributions in the Z direction when cold molecules are loaded (upper figure) and trapped (lower figure), respectively. The loading direction of the cold molecular beam is indicated by an arrow in Fig. 1. We can see from Fig. 4(a) that when it is the loading case, the field distribution in the Z direction is asymmetric, that is, the potential barrier (i.e., the right barrier) above the trapping center is lowered to nearly zero, which can be used to load the cold molecular beam into our trap. So in this case, when the cold molecules move along the $-Z$ direction, they will first experience a slowing process resulting from the gradient force of the left electrostatic field until most of them are slowed to 0 m/s, and then they will be reflected back, and when they arrive near the center of the trap, we will rapidly change the voltage U_1 and U_2 into -15 kV and 0 respectively so as to confine cold molecules in our trap. Figure 4(b) shows the contour distributions of the electrostatic field in the XOY plane at different Z positions. We can infer that in the process of loading, the molecules always feel a transverse force that prevents the divergence of the molecules in the transverse directions.

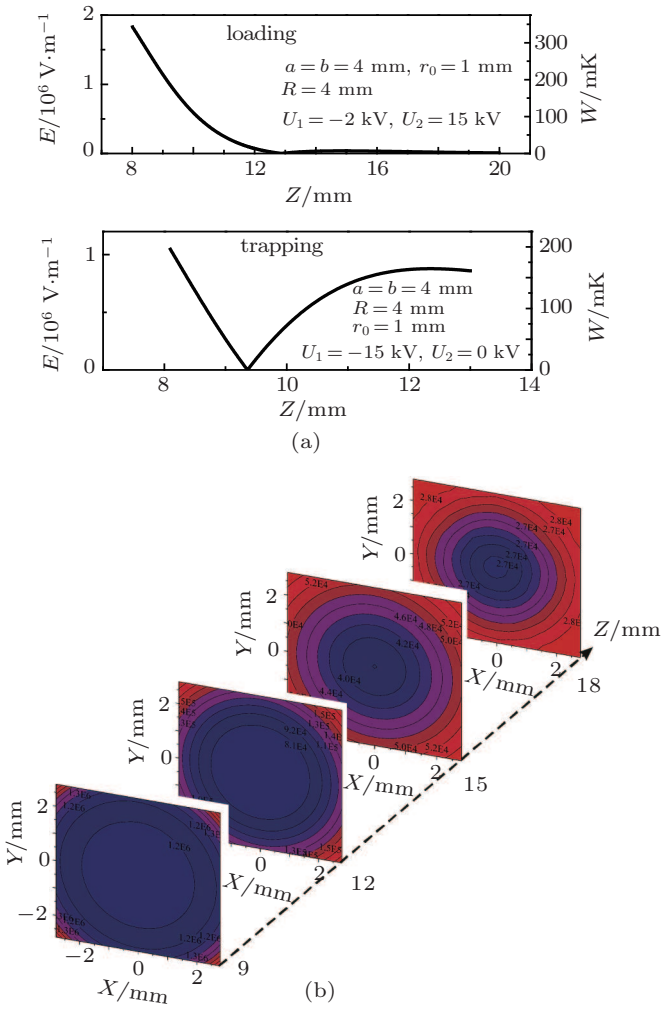


Fig. 4. (color online) (a) Electric field distribution in the Z direction in the loading and the trapping processes of cold molecules, the corresponding Stark potential for ND_3 molecules in the state $|J,KM\rangle = |1,-1\rangle$ is also given. (b) The contour distributions of the electric field in the XOY plane at different Z positions in the loading process.

Figure 5(a) shows the relationships between the loading efficiency and the loading time $t_{\rm load}$ for four different initial velocities of the incident molecular beam. The data points with the black (solid square), red (solid circle), green (solid triangle), and blue (solid inverted triangle) curves are for the initial velocities of 11 m/s, 12 m/s, 13 m/s, and 14 m/s, respectively. From Fig. 5(a), we can see that (I) the loading efficiency of cold molecules is not only related to the loading time, but also dependent on the initial velocity of incident molecular beam; (II) for a given initial velocity, there are always an optimal loading time and a maximum loading efficiency; (III) when initial velocities of incident molecular beam are 11 m/s, 12 m/s, 13 m/s, and 14 m/s, the optimal loading times are 0.909 ms, 0.865 ms, 0.8275 ms, and 0.7978 ms respectively, and the corresponding maximum loading efficiencies can reach 81.7%, 87.1%, 87.7%, and 80.4% respectively. This shows that there is a strong dependence of the maximum loading efficiency on initial velocity of incident molecular beam. For this, we further study the relationship between the maximum loading efficiency of cold molecules and the initial velocity of the incident beam, and the results are shown in Fig. 5(b). It can be seen from Fig. 5(b) that with the increase of the incident-beam velocity, the maximum loading efficiency first increases, and then reduces after reaching their corresponding maximum values. In particular, when the incident-beam velocity is 13 m/s, the maximum loading efficiency can reach about 87.7%.

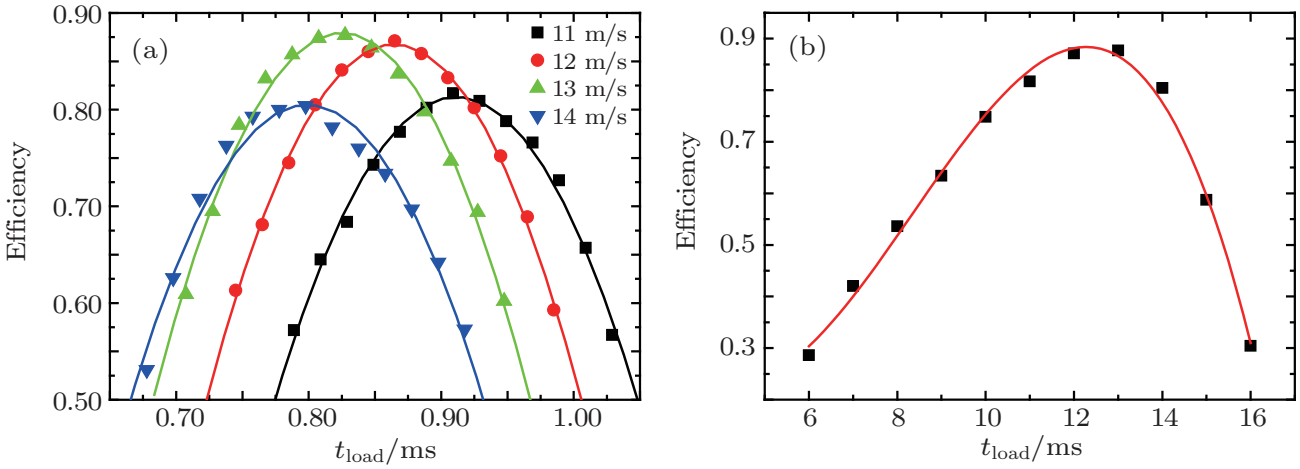


Fig. 5. (color online) (a) Variations of loading efficiency with loading time for the different velocities of the incident molecular beam. (b) Variation of maximum loading efficiency with initial velocity of incident molecular beam. The data points represent the simulated results and the solid lines are the fitted lines. The used parameters are shown in each panel.

4. An application: Adiabatic cooling

Here we use our trapping scheme to study the adiabatic cooling of the trapped ND_3 molecules by using Monte-Carlo simulations. The trapping voltage U_1 is -35 kV, and the voltage applied to the middle ring electrode is 0, and the lowest ring electrode is ground. We first load cold molecules into our surface potential-well and trap them for 500 ms, then we slowly lower the trapping voltage U_1 in steps of 1 kV, and the voltage is kept for 10 ms, then the cycle is repeated. We expect that as U_1 decreases, the dipole gradient force on the trapped molecules becomes weaker, and then the molecular cloud will be adiabatically expanded in the well, and the temperature of the molecular packet will decrease. In Figs. 6(a) and 6(b), the left panels show the contour distributions of the electrostatic field in the XOZ and XOY planes, the corresponding E-field values are shown in contours in units of V/m. From top to bottom, the trapping voltages are -3 kV, -20 kV, and -35 kV, respectively. The right panels show the corresponding spatial distributions of cold molecules in the trap. Just as we expect, when U_1 decreases the packet of cold molecules will expand in the well. We study the dependences of the temperature of the trapped molecules on the trapping voltage in the process of adiabatic expansion, and the results are shown in Fig. 6(c). We can find from Fig. 6(c) that I) with the lowering of the trapping voltage, the temperatures (including $T_{x,y}$, T_z, and $T_{\rm 3D}$) will be reduced monotonically. II) The lowering of molecular temperature in the Z direction is faster than in both the X and Y directions because the confinements of cold molecules in the X and Y directions are tighter than in the Z direction. III) When the trapping voltage U_1 is reduced from -35 kV to -3 kV, the 3D temperature of the trapped molecules will be dropped from 34.5 mK to 5.8 mK in the process of adiabatic cooling. This shows that our trap scheme can be used to realize an efficient adiabatic cooling of cold molecules by lowering the potential-well depth (i.e., by lowering the trapping voltage U_1).

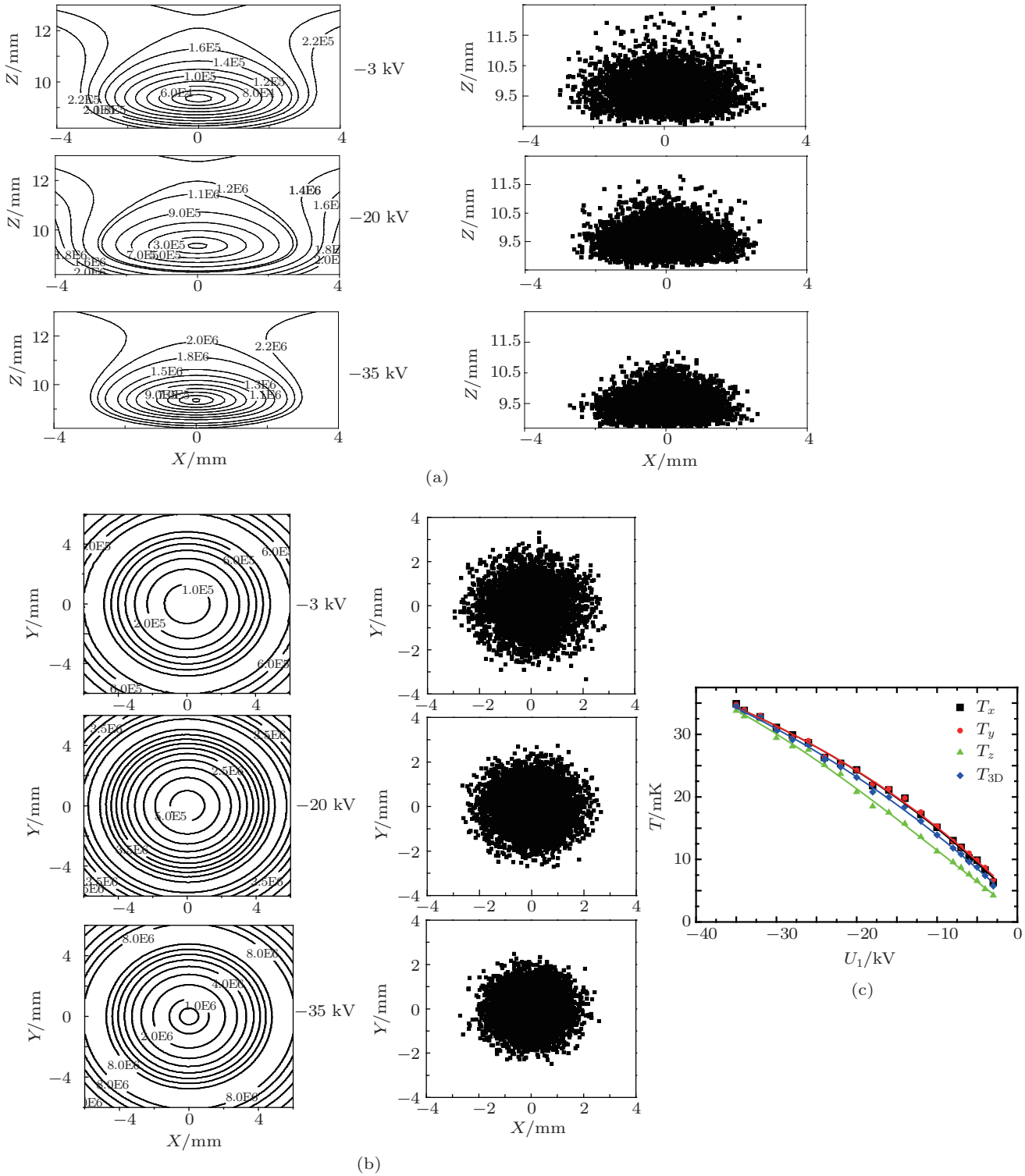


Fig. 6. On the left side, contour distributions of the electrostatic field in the (a) *XOZ* and (b) *XOY* planes, with the trapping voltages being −3 kV, −20 kV, and −35 kV and the corresponding *E*-field values in contours being in units of V/m. On the right side, the corresponding spatial distributions of cold molecules in the trap. (c) The dependences of the temperatures (including $T_{x,y}$, T_z, and T_{3D}) of trapped molecules on trapping voltage in the process of adiabatic expansion. In panels (a) and (b), the electrostatic field is expressed in the form of 1.6E5, which means 1.6×10^5.

5. Conclusions

We propose a novel scheme for trapping cold WFS molecules by using two insulator-embedded charged rings and a grounded conductor plate, and numerically calculate the spatial distributions of the electrostatic field generated by our charged-ring layout and its Stark trapping potential for ND_3 molecules. We find that the position of the trapping center above the chip and its efficient well depth can be controlled conveniently by changing the value of U_2 on the charged ring 2. We also perform the Monte–Carlo simulations for the

loading and trapping processes of cold ND_3 molecules in the state $|J,KM\rangle = |1,-1\rangle$, and study the dependences of the loading efficiency on both the loading time and the initial velocity of the incident molecular beam. Our results show that the loading efficiency of our trapping scheme can reach up to 87.7% when the initial velocity of the molecular beam is 13 m/s, and the corresponding optimal loading time is 0.8275 ms. We also investigate the adiabatic cooling of cold molecules in our surface trap scheme by lowering its trapping voltage, and find that our trap scheme can be used to realize an efficient adiabatic cooling of the trapped molecules. It is clear that such a controllable high-efficiency electrostatic surface trap can be used to form various integrated molecule chips, and study cold collisions and cold chemistry on a chip and the reduction of the trapping lifetime due to the interaction of cold molecules with the chip surface, even can be studied as a function of molecular temperature and distance from the surface. With cold molecules trapped in an electrostatic well for up to seconds, we can study the lifetimes of the electronic or vibrational excited states.[36,37] Trapped polar molecules also hold promise for use in quantum information systems.[38]

References

[1] Schnell M and Meijer G 2009 *Angew. Chem. Int. Ed.* **48** 6010
[2] Friedrich B and Doyle J M 2009 *ChemPhysChem* **10** 604
[3] van de Meerakker S Y T, Bethlem H L, Vanhaecke N and Meijer G 2012 *Chem. Rev.* **112** 4828
[4] Lemeshko M, Krems R V, Doyle J M and Kais S 2013 *Mol. Phys.* **111** 1648
[5] Hogan S D, Motsch M and Merkt M 2011 *Phys. Chem. Chem. Phys.* **13** 18705
[6] Veldhoven J V, Kupper J, Bethlem H L, Sartakov B, vanRoij A J A and Meijer G 2004 *Eur. Phys. J. D* **31** 337
[7] Filsinger F, Erlekam U, Von Helden G, Kupper J and Meijer G 2008 *Phys. Rev. Lett.* **100** 133003
[8] Gilijamse J J, Hoekstra S, vande Meerakker S Y T, Groenenboom G C and Meijer G 2006 *Science* **313** 1617
[9] Willitsch S, Bell M T, Gingell A D, Procter S R and Softley T P 2008 *Phys. Rev. Lett.* **100** 043203
[10] Otto R, Mikosch J, Trippel S, Weidemuller M and Wester R 2008 *Phys. Rev. Lett.* **101** 063201
[11] Shuman E S, Barry J F and DeMille D 2010 *Nature* **467** 820
[12] Hummon M T, Yeo M, Stuhl B K, Collopy A L, Xia Y and Ye J 2013 *Phys. Rev. Lett.* **110** 143001
[13] Thorscheim H R, Weiner J and Julienne P S 1987 *Phys. Rev. Lett.* **58** 2420
[14] Lett P D, Helmerson K, Phillips W D, Ratliff L P, Rolston S L and Wagshul M E 1993 *Phys. Rev. Lett.* **71** 2200
[15] Miller J D, Cline R A and Heinzen D J 1993 *Phys. Rev. Lett.* **71** 2204
[16] Ni K K, Ospelkaus S, de Miranda M H G, Peer A, Neyenhuis B, Zirbel J J, Kotochigova S, Julienne P S, Jin D S and Ye J 2008 *Science* **322** 231
[17] Lang F, Winkler K, Strauss C, Grimm R and Hecker D J 2008 *Phys. Rev. Lett.* **101** 133005
[18] Danzl J G, Haller E, Gustavsson M, Mark M J, Hart R, Bouloufa N, Dulieu O, Ritsch H and Nagerl H C 2008 *Science* **321** 1062
[19] Campbell W C, Groenenboom G C, Lu H I, Tsikata E and Doyle J M 2008 *Phys. Rev. Lett.* **100** 083003
[20] Weinstein J D, De Carvalho R, Guillet T, Friedrich B and Doyle J M 1998 *Nature* **395** 148
[21] Rangwala S A, Junglen T, Rieger T, Pinkse P W H and Rempe G 2003 *Phys. Rev. A* **67** 043406
[22] Bethlem H L, Berden G and Meijer G 1999 *Phys. Rev. Lett.* **83** 1558
[23] Bethlem H L, Berden G, Crompvoets F M H, Jongma R T, van Roij A J A and Meijer G 2000 *Nature* **406** 491
[24] Hudson E R, Ticknor C, Sawyer B C, Taaties C A, Lewandowski H J, Bochinski J R, Bohn J L and Ye J 2006 *Phys. Rev. A* **73** 063404
[25] Hou S Y, Li S Q, Deng L Z and Yin J P 2013 *J. Phys. B: At. Mol. Opt. Phys.* **46** 045301
[26] Yamakita Y, Procter S R, Goodgame A L, Softley T P and Merkt F 2004 *J. Chem. Phys.* **121** 1419
[27] Vanhaecke N, Meier U, Andrist M, Meier B H and Merkt F 2007 *Phys. Rev. A* **75** 031402
[28] Hogan S D, Sprecher D, Andrist M, Vanhaecke N and Merkt F 2007 *Phys. Rev. A* **76** 023412
[29] Hogan S D, Wiederkehr A W, Schmutz H and Merkt F 2008 *Phys. Rev. Lett.* **101** 143001
[30] Barker P F and Shneider M N 2002 *Phys. Rev. A* **66** 065402
[31] Fulton R, Bishop A I, Shneider M N and Barker P F 2006 *Nat. Phys.* **2** 465
[32] Elioff M S, Valentini J J and Chandler D W 2003 *Science* **302** 1940
[33] Liu N N and Loesch H 2007 *Phys. Rev. Lett.* **98** 103002
[34] Moon P B, Rettner C T and Simons J P 1978 *J. Chem. Soc. Faraday Trans.* **74** 630
[35] Bethlem H L, Crompvoets F M H, Jongma R T, van de Meerakker S Y T and Meijer G 2002 *Phys. Rev. A* **65** 053416
[36] van de Meerakker S Y T, Vanhaecke N, van der Loo M P J, Groenenboom G C and Meijer G 2005 *Phys. Rev. Lett.* **95** 013003
[37] Gilijamse J J, Hoekstra S, Meek S A, Metsala M, van de Meerakker S Y T, Meijer G and Groenenboom G C 2007 *J. Chem. Phys.* **127** 221102
[38] Andre A, DeMille D, Doyle J M, Lukin M D, Maxwell S E, Rabl P, Schoelkopf R J and Zoller P 2006 *Nat. Phys.* **2** 636
[39] Bethlem H L, Berden G, Crompvoets F M H, Jongma R T, van Roij A J A and Meijer G 2000 *Nature* **406** 491
[40] van Veldhoven J, Bethlem H L, Schnell M and Meijer G 2006 *Phys. Rev. A* **73** 063408
[41] Hendrick L B, van Veldhoven J, Melanie Schnell and Meijer G 2006 *Phys. Rev. A* **74** 063403
[42] Rieger T, Junglen T, Rangwala S A, Pinkse P W H and Rempe G 2005 *Phys. Rev. Lett.* **95** 173002
[43] Leinert J K, Haimberger C, Zabawa P J and Bigelow N P 2007 *Phys. Rev. Lett.* **99** 143002
[44] Buhmann S Y, Tarbutt M R, Scheel S and Hinds E A 2008 *Phys. Rev. A* **78** 052901
[45] Meek S A, Conrad H and Meijer G 2009 *Science* **324** 1699
[46] Ma H, Zhou B, Liao B and Yin J P 2007 *Chin. Phys. Lett.* **24** 1228
[47] Wang Q, Li S Q, Hou S Y, Xia Y, Wang H L and Yin J P 2014 *Chin. Phys. B* **23** 013701
[48] Zare R N 1987 *Angular Momentum* (New York: John Wiley & Sons) p. 177